THE JOURNAL OF PHYSICAL CHEMISTRY C

ARTICLE

pubs.acs.org/JPCC

Understanding the Behavior of New Plasmonic Probes with Sub-Nanometric Resolution in Field Enhanced Scanning Optical Microscopy

Eduardo M. Perassi,[†] Alberto F. Scarpettini,[‡] Martín E. Masip,[‡] Andrea V. Bragas,[‡,§] and Eduardo A. Coronado[†,*]

[†]INFIQC. Centro Láser de Ciencias Moleculares, Dpto. de Fisicoquímica, Facultad de Ciencias Químicas, Universidad Nacional de Córdoba, Suc. 16, C.C. 61, 5016, Córdoba, Argentina

[‡]Laboratorio de Electrónica Cuántica, Departamento de Física, Facultad de Ciencias Exactas y Naturales, Universidad de Buenos Aires, Pabellón 1, Ciudad Universitaria, 1428 Buenos Aires, Argentina

[§]IFIBA. Consejo Nacional de Investigaciones Científicas y Tecnológicas, CONICET. Argentina

ABSTRACT: Recently, using field enhanced scanning optical microscopy (FESOM), a new kind of plasmonic nanostructured probes has been introduced capable to achieve subnanometric vertical resolution on atomically flat samples. These plasmonic probes consisting in silica (SiO_2) microspheres decorated with 5 nm diameter spherical Ag nanoparticles (NPs) exhibit a multiple peaked experimental extinction spectra in colloidal dispersion. The subnanometric resolution achieved in FESOM is observed when they are attached to a metal tip and illuminated at 632 nm. On the contrary, these probes lack of resolution in FESOM measurements upon 532 nm laser light illumination. In this work, the complex extinction properties of these probes as well as their near field optical properties are compared and analyzed by means of rigorous electrodynamic simulations. The calculations show that the far and near field optical behavior can only be explained in a consistent way in terms of the plasmonic response of small Ag NPs clusters on the silica surface. Using these cluster configurations, the near field simulations of the optical response are also found to be in excellent agreement with the experimental FESOM approach curves, demonstrating in this way the subnanometric resolution achieved at 632 nm and the almost null response at 532 nm.

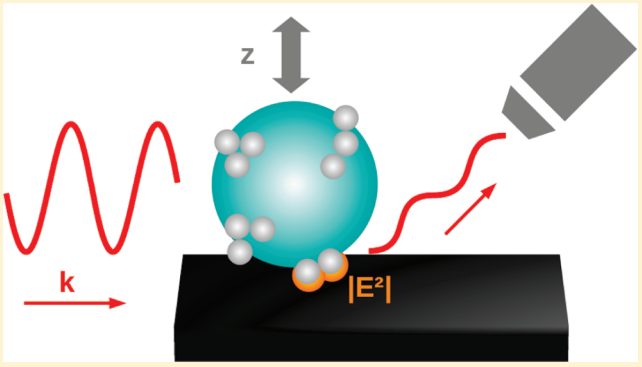

1. INTRODUCTION

Design of nanostructures able to provide a strong field enhancement and confinement is today at the focus of the nano-optics field. The challenge is to go back and forth from the experimental realization to the modeling,[1−3] to obtain nano-objects, which simultaneously maximizes low time-cost fabrication and wide applicability for a given purpose. Just as the promising single molecule plasmonic sensors[4,5] and substrates for SERS (surface enhanced raman spectroscopy)[6] are based on a smart engineering of nanoobjects,[7] microscopy at the nanoscale follows similar roads, with the aim to be a versatile and sensitive tool in a nanoscience fast development scenario.

Field enhanced scanning optical microscopy (FESOM)[8,9] and NanoRaman[10,11] relies on the fabrication of probes, which provide enough enhancement of the near field around the probe, surpassing the background light and supplying optical and chemical contrast at the nanometric scale.[12] Although the most widely used enhancers in near field optical microscopy are the metal-evaporated dielectric tips,[13−17] in recent years design of metal NPs based probes[8,18−21] has been considered a better choose to increase the optical resolution of these techniques, keeping a good compromise between easy fabrication and performance.

In a previous work, we have introduced new plasmonic probes built with NP-decorated silica microspheres, which showed subnanometric optical vertical resolution over an atomically flat sample.[8] Besides the great resolution these probes are able to reach, the spectral behavior of these structures deserves special attention because the resonances of the probes determine the light frequency at which it is worth to work to achieve the highest possible resolution. In this article, we aim to understand how the plasmonic properties of these complex structures determines the subnanometric resolution in FESOM,[8] by comparing the experimental results with simulations made using two electrodynamics approaches: generalized multiparticle Mie theory (GMM)[22,23] and the discrete dipole approximation (DDA).[24,25] We show that

Received: February 21, 2011
Revised: April 15, 2011
Published: May 12, 2011

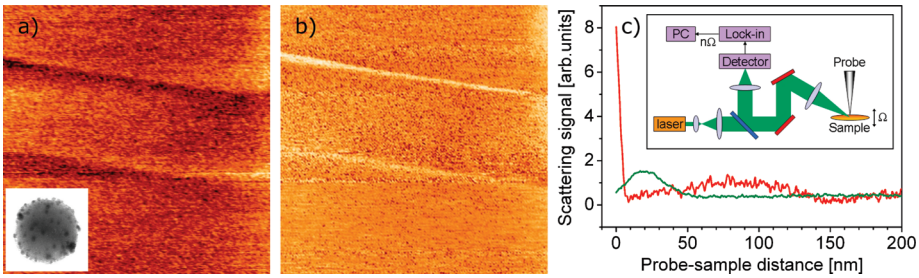

Figure 1. a) Optical image of graphite (HOPG), taken with the field enhancement scanning optical microscope (FESOM). Two steps of less than 1 nm in height are clearly visible. Size of the image: 560 × 560 nm^2. The insert shows the TEM image of a microsphere of 170 nm of diameter decorated with 5 nm Ag Nps. b) STM image in constant height mode of the same region. c) Approach curves, showing the backscattered light as a function of the probe-sample distance in FESOM. Red curve is the measurement using 632 nm laser light, whereas the green curve accounts for the 532 nm illumination. In the insert, a scheme of the experimental setup is shown.

the nontrivial structure of the probes extinction spectra measured in colloidal dispersion can be explained by the plasmonic interaction of two and three Ag NPs with little different spatial morphologies at the surface of the microsphere. The presence of these Ag clusters on the silica microsphere is able to explain the near field optical behavior of these plasmonic probes, and therefore the optimum resolution obtained at 632 nm and the almost null optical contrast obtained at 532 nm, these facts are accounted for mapping the electromagnetic field enhancement at the two wavelengths used in the FESOM experiments.

2. EXPERIMENTAL METHODS

2.1. Probes in Solution. The experimental procedure for the NP-decorated silica microspheres preparation is comprehensively described in previous work.[8] In short, Ag NPs of 5 nm of average diameter, covered by aminosilane molecules (*N*-[3-(trimethoxysilyl)propyl]diethylenetriamine), attach to the surface of a colloidal dispersion of silica spheres (with diameters in the range 100−200 nm) after mixing both aqueous solutions for several hours. Relative concentrations have been chosen to be 3000 Ag Nps per silica microspheres. However, not all the NPs will be adsorbed on the spheres surfaces, and thus many of them will be still in solution after the decoration procedure. A commercial Shimadzu UV−vis spectrometer was used to measure the extinction spectra of the probes in solution.

2.2. Probes for FESOM. A silver wire was immersed for 10 min in the NP-decorated colloidal dispersion as described in detail previously.[8] Probes got adsorbed on the surface of the wire, which is used as the tip for FESOM measurements.

2.3. FESOM. The field enhanced scanning optical microscopy technique is described elsewhere.[8,9] Basically, the probe-sample junction is side-illuminated with lasers at various light wavelengths, and the scattered light is collected in a backscattering configuration with a pin-photodiode detector. Lockin detection is performed by dithering the sample few angstroms in the direction of its normal with a piezo, and performing a harmonic detection[26,27] to improve the signal-to-noise ratio. Feedback mechanism, when necessary, is provided by the simultaneously recorded tunneling current.

2.4. Approach Curves. The approach curve is the plot of the backscattered light as a function of the probe-sample distance recorded by the FESOM. With the feedback loop totally turned off, a ramp of voltage is applied to the z-piezo, which moves the sample toward the probe from large distances (several wavelengths) until a given tunneling current is detected, followed by the retraction of the piezo. The probe−sample distance for which the preset tunneling current is reached, is defined as an arbitrary zero of distance in these curves.

3. THEORETICAL CALCULATIONS

3.1. DDA Simulations with a Random Coverage of Ag Nanospheres on the Microsphere. The DDA method[24,25] has been described several times. Shortly, the DDA replaces the solid particle by an array of N point dipoles, with the spacing between the dipoles small compared to the wavelength. Each dipole has an oscillating polarization in response to both an incident plane wave and the electric fields due to all of the other dipoles in the array. The innovation we have implemented in this work is the target generation, since we have decorated in a random fashion, a microsphere with Ag NPs. This scheme intends to simulate more accurately the experimental situation. Random numbers were generated to locate the NPs on the microsphere surface. To obtain the highest degree of coverage, several seeds numbers were used and also the initial number of spheres on the surface was chosen arbitrary among the structures already generated in a given decoration simulation. At low degrees of coverage, this procedure is fast but, as the number of NPs increases, it takes a much larger number of trials. Using this random procedure, we were able to decorate a 100 nm microsphere with 900 NPs of 5 nm diameter. The DDA simulations were performed using a grid spacing of 0.75 nm. The dielectric constant from Palik[28] was used for Ag, whereas all of the nanostructure was supposed to be immersed in a medium with a constant refractive index equal to 1.47.

3.2. Generalized Multiparticle Mie Theory (GMM). The extinction spectrum of the NP clusters was computed using the generalized multiparticle Mie theory (GMM).[22,23] This is an analytical method able to solve, in a rigorous and exact way, the complex problem of interaction between an electromagnetic field and an aggregate of spheres. The GMM method has been described elsewhere so we will give a brief summary here. In the GMM method, scattered fields from each one of the L individual spheres are solved in terms of the respective sphere-centered reference systems. In an arbitrarily chosen primary jth coordinate system, the Cartesian coordinates of the origins of these L displaced coordinate systems (i.e., the sphere centers) are (Xj, Yj, Zj), $j = 1, 2,..., L$. To solve multisphere-scattering through the Mie-type multipole superposition approach, the incident plane wave is expanded in terms of vector spherical wave functions in each of the L sphere-centered coordinate system. Similar to the incident field, individual scattered field of the each

dx.doi.org/10.1021/jp201717f |*J. Phys. Chem. C* 2011, 115, 10455–10461

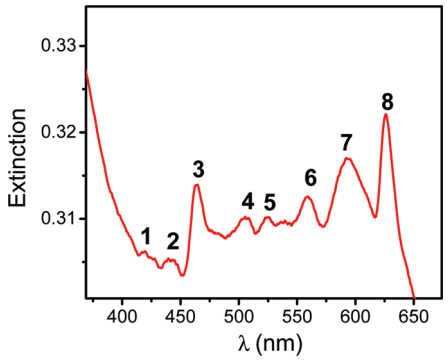

Figure 2. Experimental extinction spectra of the silica microspheres decorated with Ag NPs in colloidal dispersion.

component spheres is expanded in terms of vector spherical wave functions in each of the L sphere-centered coordinate system. Then the boundary conditions are solved for the partial scattering coefficients. Finally, referring an arbitrarily located common coordinate system, the total scattering is expanded in term of vector spherical wave function and it is related to the partials scattering by a simple phase term. With the total scattered field, and based on the analytical expressions for amplitude scattering matrix of an aggregate of spheres, it is possible to derive rigorous formula for other fundamental scattering properties such as extinction, absorption, and scattering cross sections.[22,23] As in the DDA simulations in all of the calculations presented, the Ag clusters were immersed in a uniform dielectric environment with refractive index 1.47 and the dielectric function tabulated by Palik for Ag was employed.[28]

4. RESULTS AND DISCUSSION

4.1. FESOM Plasmonic Probes and Image Performance. Part a of Figure 1 shows a high-resolution optical image of graphite (HOPG) taken with FESOM using the plasmonic probes described in the experimental section. As a reference, we include in part b of Figure 1 the constant-height STM image, recorded simultaneously with the FESOM image. Two graphite steps are clearly seen, whose heights have been measured with the help of a constant-current STM image recorded at the same place, giving heights of less than 1 nm. The FESOM image has been taken by illumination with red light at 632 nm. This high subnanometric optical resolution obtained deserves to be analyzed by a careful analysis of the plasmonic nanostructures responsible for this high optical contrast.

In part c of Figure 1, the approach curves are shown, accounting for the backscattered light as a function of probe-sample distance. The field enhancement effect at very short probe-sample distance is evident when red laser light (632 nm) impinges the junction. However, illumination with green laser light (532 nm) produces no contrast in the optical image, and, as a consequence, the approach curve tends to zero for very small distances.

4.2. Far Field Optical Properties of the Plasmonic Probes. To understand the optical response of these FESOM plasmonic probes, it is first necessary to understand their far field optical behavior. The experimental UV−vis spectra of the Ag NP-decorated microspheres in colloidal dispersion (before to attach them to the metal tip) depicts a complicated multiple peaked spectra, as shown in Figure 2. The most prominent peaks labeled 3, 7, and 8 correspond to λ = 464, 594, and 626 nm respectively, the peaks with

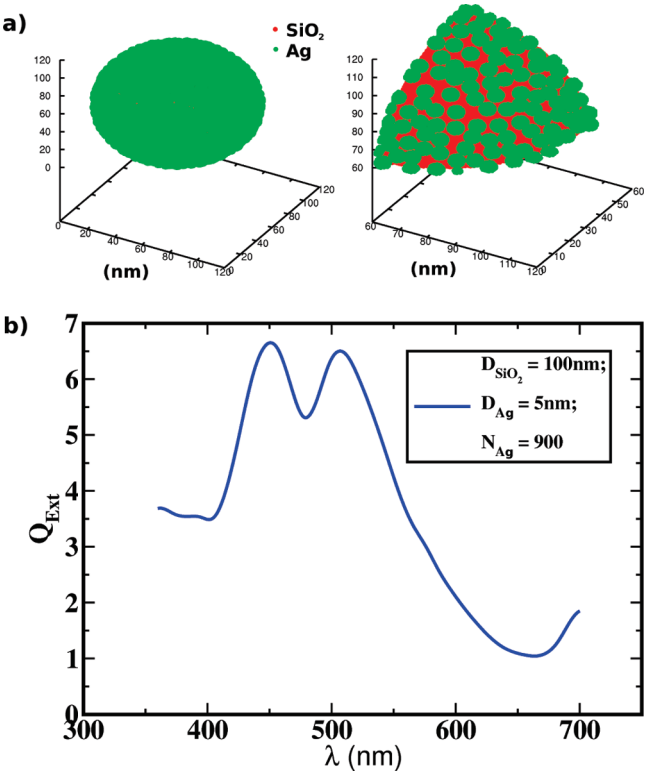

Figure 3. DDA simulations of 5 nm spherical Ag NPs randomly distributed on a microsphere. a) On the left it depicts a typical example of a random location of 900, 5 nm diameter Ag nanospheres, on 100 nm diameter microsphere, whereas, on the right a smaller portion of the microsphere surface is shown. b) Shows the calculated extinction spectra corresponding to the nanostructure in panel a).

moderate intensity labeled 4 and 6 occur at λ = 505 nm and 559 nm respectively, and there are a series of peaks with weak intensity labeled 1, 2, and 5 at λ = 418, 441, and 525 nm, respectively. At short wavelengths, the spectra exhibits a decay that can be assigned to the light scattered by the silica microspheres.

In a first attempt to explain these complicated spectral features, we assumed that the Ag nanospheres were distributed in a random way around the silica surface. Using a random target generator (explained in the methodology section) and after several thousands of iterations, the surface of a 100 nm diameter silica microsphere was covered with 900, 5 nm diameter Ag Nps, reaching in this way almost the highest degree of coverage possible. At this point, increasing the number of iterations did not produce any change in the number of NPs on the silica surface, which means that the probability to find room for a additional Ag NP here on the surface is very low. Part a of Figure 3 shows the spatial configuration obtained after covering the silica surface with 900 Ag NPs in the random way described above; the right panel depicts a zoom view of the NPs on the silica surface. Note that the electrostatic interaction of NPs or the presence of molecules acting as fixed length separator between them were not taken into account in this simulation; only the geometrical constrains dominates the final configuration of the NPs.

Simulating the real experimental situation would also require to perform the average of the optical response over all the possible configurations of randomly placed NPs on the microsphere surface, but this is indeed an impossible task. However, as it will be shown later, this would not be necessary. The calculated extinction

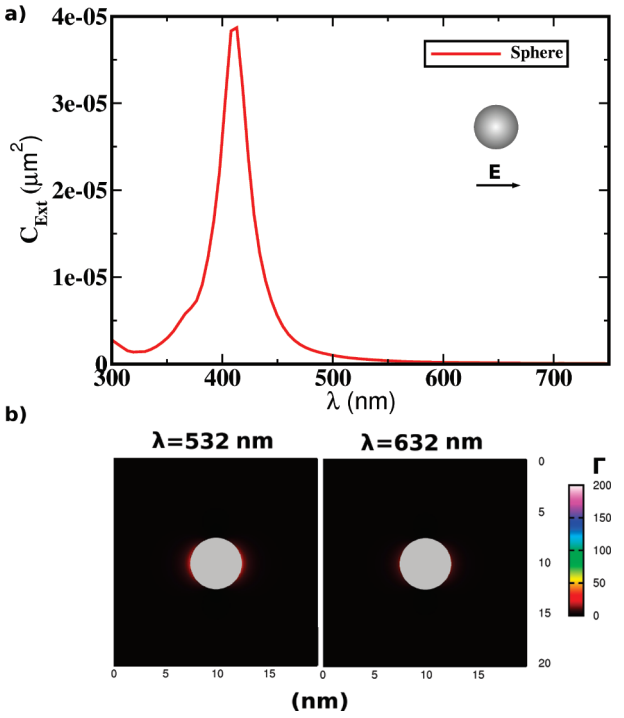

Figure 4. a) Calculation of the extinction spectra of a 5 nm diameter Ag sphere immersed in a dielectric media with n = 1.47. The incident polarization is indicated by a scheme on the right. b) Near field enhancement map calculated using GMM theory of the single Ag NP shows in a) at the two wavelengths used in the FESOM experiments.

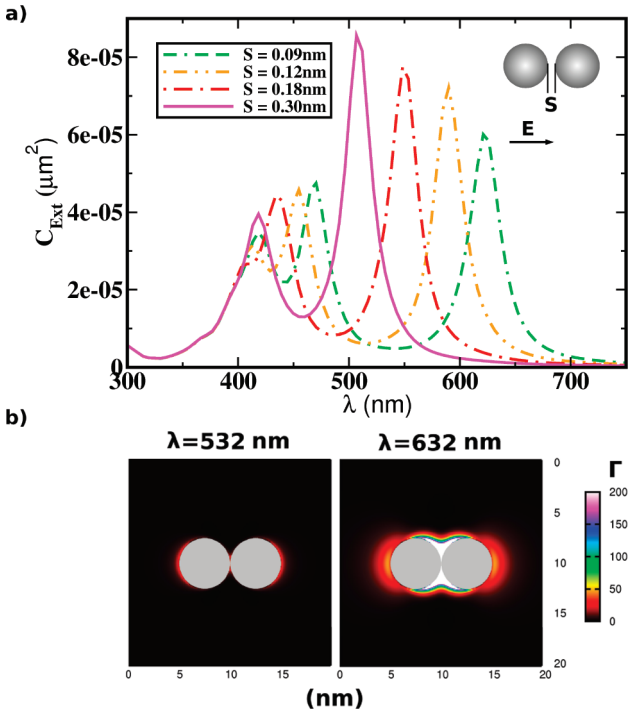

Figure 5. a) GMM calculated extinction spectra of 5 nm diameter Ag dimers immersed in a dielectric media with n = 1.47 at different interparticle separations as indicated in the insert. The incident polarization is indicated by a scheme on the right. b) Near field enhancement calculated using GMM theory for the Ag dimer shown in a) at the two wavelengths used in the FESOM experiments, for a dimer interparticle separation S = 0.09 nm.

shown in part b of Figure 3, probed to be broad and double peaked which is quite usual in large clusters.[29] Therefore, this DDA simulation performed with high degree of random coverage on the silica surface was not able to explain the multiple peaks observed in the extinction experiments. Another series of simulations (not shown) with high degree of coverage but with a different random distribution were performed, but in all of them the same general features of the spectra shown in part b of Figure 3 were obtained.

Although these simulations were unsuccessful, an inspection of the random process used to decorate the silica microsphere probed to be quite useful to give a clear picture of the decoration process. Under the assumption that no diffusion process is taking place after each NP deposition, it was observed at the early stages of the decoration, that is low coverage, that single non interacting spheres structures were the most probable structures. As the number of NPs deposited increased, the presence of many dimers and some trimers were evidenced (i.e., spheres with interparticle distances less than 0.3 nm), being the dimer by far more frequent than the trimer.[30]

On the basis of these results, it was reasonable to think that the observed optical behavior was due to the presence of these clusters formed at relatively low degree of coverage on the silica microsphere. These clusters should mainly be formed by two Ag NPs, to a lesser extent by three Ag NPs, and with a very small probability, by more than three NPs, at the particular values of interparticle separation mentioned above. Taking into account these configurations observed in the random decoration process, we analyzed the optical behavior of the following nanostructures: single spheres, dimers and three types of trimers (linear trimer, L-shaped trimer, and V-shaped trimer); the geometries are depicted in the schemes inserted in part a of Figures 4, part a of 5, and parts a−c of 6. The simulations were performed using GMM theory, as described in the methodology section. In these calculations the spheres were considered to be in a uniform dielectric environment with refractive index n = 1.47 because the spheres were covered with an *N*-[3-(trimethoxysilyl)propyl]diethylenetriamine (ATS) layer, whose refractive index almost matches the refractive index of silica. This assumption was corroborate by computing the extinction spectra of a 5 nm diameter Ag sphere in a media with n = 1.47 as shows in part a of Figure 4, which depicts a peak at 410 nm in good agreement with experiments.[31]

The GMM simulations for Ag dimers at different edge to edge separation S, corresponding to S = 0.09, 0.12, 0.18, and 0.30 nm (green, yellow, red, and pink lines, respectively) are shown in part a of Figure 5. Although these S values are arbitrary ones, it is found that at S = 0.09 nm which correspond to a NP pair of almost touching spheres, the extinction spectra matches the two more intense peaks labeled 3 and 8 and also the less prominent peak 1 (Figure 2). The configuration with S = 0.12 nm, results in an extinction spectra with resonances at almost the same wavelength than peaks labeled 7, 3, and 1. The extinction spectra of the dimer with S = 0.18 reproduce the peaks 6, 2 and 1; and the one with S = 0.30 nm reproduces the peaks 4 and 1. It is important to note the peak labeled 1 was obtained only when more than one NP are interacting as it would also be demonstrated for trimers below.

Parts a−c of Figure 6 show the extinction spectrum for trimers aggregates (linear, L-shaped, and V-shaped) at the same values of S than before that is S = 0.09 nm, S = 0.12 nm, S = 0.18 nm,and S = 0.3 nm. The most intense peak labeled 3 in Figure 2 can be assigned either to the linear trimer with S = 0.12 nm or the

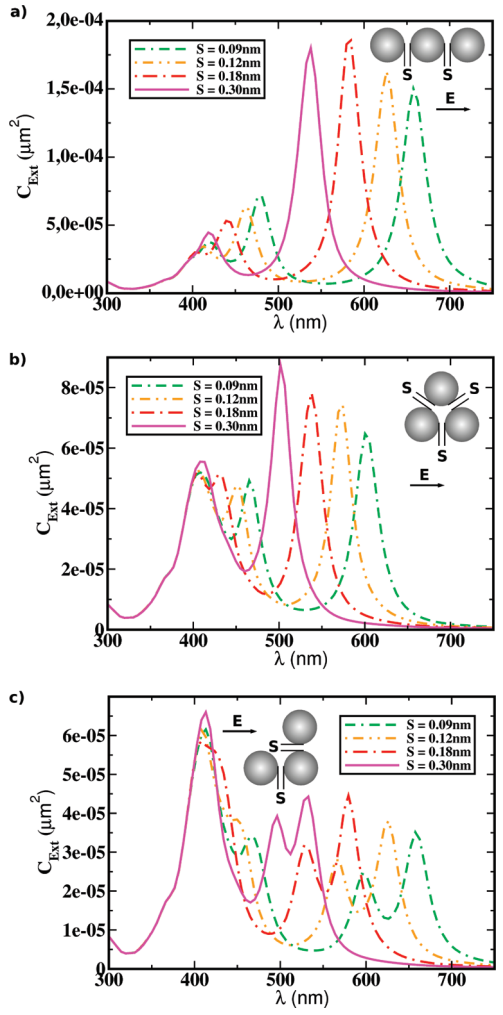

Figure 6. GMM calculated extinction spectra of 5 nm diameter Ag NP arranged in a) a linear trimer, b) a V-shaped trimer, and c) an L-shaped trimer, immersed in a dielectric media with n = 1.47 at different interparticle separations as indicated in the insert. The incident polarization is indicated by the inserted scheme.

V-shaped and L-shaped trimers with S = 0.09 nm (parts a−c of Figure 6). The other intense peak labeled 8 corresponds to the linear or L-shaped trimers with S = 0.12 nm (parts a and c of Figure 6). The other plasmon resonances calculated for all the trimer configurations could explain the presence of the other peaks observed in the measured extinction spectra. Therefore, we conclude that only for very small interparticle separation in the clusters (the NPs are almost touching) the most intense peaks labeled 3 and 8 can be reproduced. As these peaks are the most intense, it is reasonable to think that the clusters where the NPs are almost touching are the most probable ones. However, as the population of all of the clusters configurations is unknown it is not possible to give a one to one correspondence between simulations and each of the observed experimental peaks, and it is only correct to say that some small clusters with specific interparticle separations are responsible of the peaked spectrum measured.

Note that the distances between NPs should be not assigned to any atomistic structure nor a chemical bond. These distances are intrinsic to the electrodynamics continuum model used for the calculation. The degree of coupling between the nanospheres of a homodimer is correlated with a sigma parameter, which is the ratio of the center to center distance of the nanospheres and the nanosphere diameter. A strong coupling between nanospheres correspond to a sigma value close to one. For example, for a given value of sigma (degree of coupling) close to one the distance S between nanospheres will be large (about 1 nm) for nanospheres with large diameter (about 50 nm)[32] but for nanospheres with rather small diameters as in the present work (5 nm) the distance S will be very short (about 0.1 nm). It follows that our approach only indicates that the real atomistic structure should be close to almost spherical structures (because perfect spheres cannot be obtained in the atomistic description of these nanoparticles) very close to each other.

4.3. Near Field Response of the Plasmonic Probes. As it can be appreciated from part c of Figure 1, the approach curves show a slight modulation of the signal at long distances, on the order of the light wavelength. This slight modulation can be assigned to the interference of the tip when it is approaching to the sample and enter within the volume of the spot of the laser. In the case that the excitation is performed with λ = 532 nm, the signal suddenly grows up at a probe-sample distance of 40 nm, until starts to decrease at a distance of about 20 nm, whereas for excitation at λ = 632 nm, it suddenly grows up very fast at a distance of about 5 nm. The behavior on the range of tens of nanometers of the plasmonic probe excited with green light is difficult to be explained in terms of a near field enhancement nearby the 5 nm diameter Ag NPs clusters, as the magnitude of the enhancement decreases almost exponential with the distance to the NPs surface. Therefore, the behavior at these distances is probably due to the light scattered by probe tip within the volume of the spot of the laser near the sample. Furthermore, the absolute magnitude of the scattering is much higher for the red than for the green light and the contrast in the images is lost for the 532 nm illumination.

The intensity of light as the plasmonic probe approaches the substrate at small distances, that is less than 5 nm, can be accounted for by our simulations performed at 532 and 632 nm for the different nanostructures analyzed in the previous section. Let us consider the near field enhancement map generated by each nanostructure at the two experimental wavelengths used to illuminate the plasmonic probes. Note that the near field enhancement at a given point will be defined as the ratio between the square modulus of the field at this point and the square modulus of the incident field, that is ($\Gamma = E^2/E_o^2$). Consider first the enhancement produced by a single sphere, whose enhancement pattern is shown in part b of Figure 4 at both wavelengths. This single NP depicts the smallest enhancement of all the nanostructures considered here, an expected result since at both wavelengths the Ag sphere is out of resonance at 410 nm. At this stage, we conclude that single isolate Ag spheres on the silica surface can not account for the near field response and it should be the presence of small clusters on this surface that originates the experimental FESOM response.

Now, the question which arises is which of the cluster configurations should be considered. As it has been shown in the previous section the most probable interparticle distance able to explain the most prominent peaks in the extinction spectra is S = 0.09 nm, therefore hereafter this interparticle distance will be used for all the calculations. From the three peaks depicted in the calculated extinction spectra (part a of Figure 5) of the Ag dimer, only one with a maximum at 626 is almost on resonance with the excitation at 632 nm used in the experiment, generating a very significant near field enhancement as shown in part b of Figure 5.

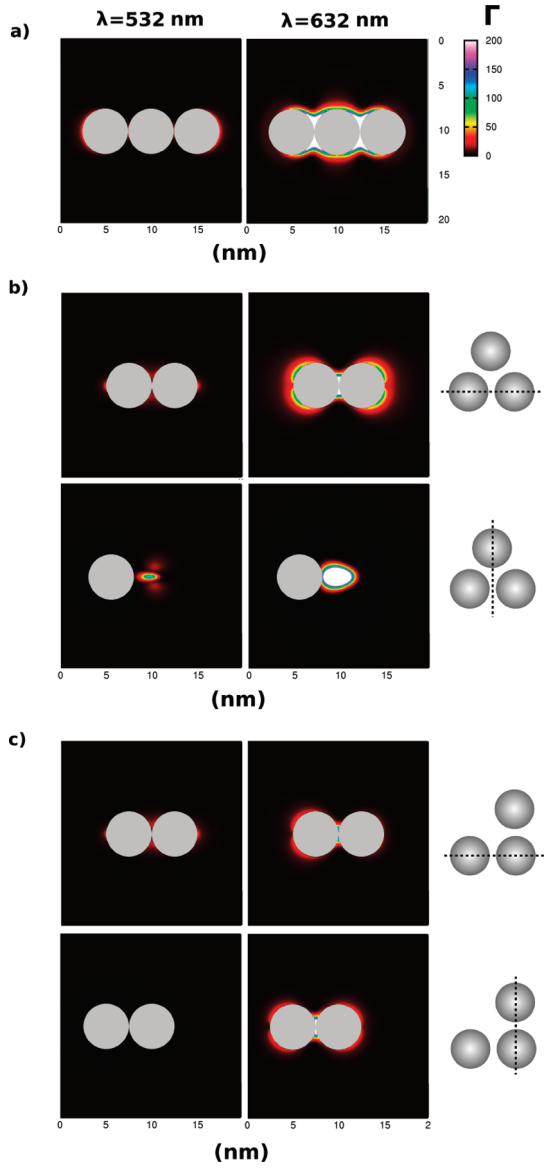

Figure 7. Near field enhancement calculated using GMM theory for the Ag trimers shown in Figure 6 at the two wavelengths used in the FESOM experiments, for interparticle separation $S = 0.09$ nm. The dashed lines on the right insert indicate for each configuration the plane where the enhanced field is plotted. a) linear trimer, b) V-shaped trimer, c) L-shaped trimer.

This fact is consistent with the abrupt increase of the light intensity observed in the approach curve recorded at this wavelength, being by far the most significant in both magnitude and spatial range at 632 nm compared with the field calculated at 532 nm where this dimer depicts no resonance wavelength (part b of Figure 5).

For linear trimers (part a of Figure 7), the behavior is qualitative the same than for Ag dimers, regarding the fact that the enhancement is almost negligible at 532 nm and very important at 632 nm, being its magnitude even greater than that calculated for the dimer. For the V-shaped trimers part b of Figure 7 sketches the enhancement in the two planes indicated by dash lines on the right of each panel. As it is clearly shown in the upper panel, the enhancement in the plane parallel to incident polarization should have the most significant contribution to the near field behavior observed in the approach curves at 632 nm. In the lower panel, which depicts the enhancement in a perpendicular plane, the field is mostly confined within the Ag cluster and therefore it is expected that this enhancement does not play any significant role in the approach curves at the same wavelength. For excitation at 532 nm, the enhancement is almost negligible for both parallel and perpendicular planes to the incident polarization, so any significant near field response is expected at this wavelength in excellent agreement with the FESOM experiments. The enhancement maps for the L-shaped geometry trimers at each wavelength (shown in part c of Figure 7) demonstrate a negligible contribution at 532 nm and a more important contribution at 632 nm. For this last wavelength, the enhancement map along the plane perpendicular or parallel to the incident polarization could make some contribution at small distances but the lower magnitude of enhancement makes this geometry to be the one that is expected to have the less important contribution to the near field response at 632 nm.

Note that, close to the particles, the field enhancement is more confined in dimers than in trimers. Part c of Figure 1 shows that the experimental signal at 632 nm drops 1 order of magnitude in about 5 nm, measured from the point defined as zero distance. This behavior compares better with the field profiles gained for trimers in part a of Figure 7 than for dimers in part b of Figure 5. Moreover, matching experimental and theoretical curves, gives that the experimental zero distance is around 1 nm, which is totally consistent with a tunneling distance.

5. SUMMARY AND CONCLUSIONS

In summary, the experimental extinction spectra of silica microspheres decorated with Ag nanospheres exhibiting multiples peaks can be explained if the degree of coverage of the silica surface is low. In such a case, the spectral features can be accounted for in terms of small Ag NPs clusters on the silica surface at specifics interparticle separations. At low degrees of coverage, the most probable clusters on the silica surface should be dimers and some trimers of almost touching Ag NPs. This feature not only explains the far field but also the near field optical response of these plasmonic probes at both wavelengths, as it is evident from the experimental FESOM approach curves. In particular, the lack of resolution and field enhancement measured at 532 nm is in agreement with the almost negligible enhancement of all the Ag clusters geometries at this wavelength. The subnanometric resolution achieved is in very good correspondence with the near field response calculated at 632 nm for Ag dimers and trimers.

AUTHOR INFORMATION

Corresponding Author

*E-mail: coronado@fcq.unc.edu.ar.

ACKNOWLEDGMENT

This work is supported by ANPCYT PICT 2006-1594, and UBA, Programación Científica 2008-2010, Proyecto No X022. E. M.P. and E.A.C. acknowledge the financial support given by SECyT-UNC, and CONICET (PIP 112-200801-02501).

REFERENCES

(1) Perassi, E. M.; Hernandez-Garrido, J. C.; Moreno, M. S.; Encina, E. R.; Coronado, E. A.; Midgley, P. A. *Nano Lett.* **2010**, *10* (6), 2097–2104.

(2) Perassi, E. M.; Canali, L. R.; Coronado, E. A. *J. Phys. Chem. C* **2009**, *113* (16), 6315–6319.
(3) Encina, E. R.; Coronado, E. A. *J. Phys. Chem. C* **2007**, *111* (45), 6796–16801.
(4) Stewart, M. E.; Anderton, C. R.; Thompson, L. B.; Maria, J.; Gray, S. K.; Rogers, J. A.; Nuzzo, R. G. *Chem. Rev.* **2008**, *108* (2), 494–521.
(5) Haran, G. *Acc. Chem. Res.* **2010**, *43* (8), 1135–1143.
(6) Stiles, P. L.; Dieringer, J. A.; Shah, N. C.; Van Duyne, R. P. *Ann. Rev. Anal. Chem.* **2008**, *1* (1), 601–626.
(7) Cortés, E.; Tognalli, N. G.; Fainstein, A.; Vela, M. E.; Salvarezza, R. C. *Phys. Chem. Chem. Phys.* **2009**, *11* (34), 7469–7475.
(8) Scarpettini, A. F.; Pellegri, N.; Bragas, A. V. *Opt. Commun.* **2009**, *282* (5), 1032–1035.
(9) Bragas, A. B.; Martínez, O. E. *Opt. Lett.* **2000**, *25* (9), 631–633.
(10) Bailo, E.; Deckert, V. *Chem. Soc. Rev.* **2008**, *37* (5), 921–930.
(11) Pettinger, B.; Domke, K. F.; Zhang, D.; Picardi, G.; Schuster, R. *Surf. Sci.* **2009**, *603*, 1335–1341.
(12) Li, J. F.; Huang, Y. F.; Ding, Y.; Yang, Z. L.; Li, S. B.; Zhou, X. S.; Fan, F. R.; Zhang, W.; Zhou, Z. Y.; Wu, D. Y.; Ren, B.; Wang, Z. L.; Tian, Z. Q. *Nature* **2010**, *464* (7287), 392–395.
(13) Hecht, B.; Sick, B.; Wild, U. P.; Deckert, V; Zenobi, R; Martin, O. J. F.; Pohl, D. W. *J. Chem. Phys.* **2000**, *112*, 7761.
(14) Salomo, M.; Bayer, D.; Schaaf, B. R.; Aeschlimann, M.; Oesterschulze, E. *Microelectron. Eng.* **2010**, *87*, 1540–1542.
(15) Bouhelier, A.; Renger, J.b; Beversluis, M. R.; Novotny, L. *J. Microsc.* **2003**, *210* (3), 220–224.
(16) Cui, X.; Zhang, W.; Yeo, B.-S.; Zenobi, R.; Hafner, C.; Erni, D. *Opt. Express* **2007**, *15*, 8309–8316.
(17) Tarun, A.; Hayazawa, N.; Kawata, S. *Anal. Bioanal. Chem.* **2009**, *394*, 1775–1785.
(18) Vakarelski, I. U.; Higashitani, K. *Langmuir* **2006**, *22* (7), 2931–2934.
(19) Höppener, C.; Novotny, L. *Nano Lett.* **2008**, *8* (2), 642–646.
(20) Eghlidi, H.; Lee, K. G.; Chen, X.-W.; Götzinger, S.; Sandoghdar *Nano Lett.* **2009**, *9* (12), 4007–4011.
(21) Anger, P.; Bharadwaj, P.; Novotny, L. *Phys. Rev. Lett.* **2006**, *96*, 113002.
(22) Fuller, K. A.; Kattawar, G. W. *Opt. Lett.* **1988**, *13* (2), 90–92.
(23) Xu, Y.-L.; Gustafson, B.Å.S. *Journal of Quantitative Spectroscopy and Radiative Transfer* **2001**, *70* (4−6), 395–419.
(24) Purcell, E. M.; Pennypacker, C. R. *Astrophys. J.* **1973**, *186*, 705.
(25) Draine, B. T.; Lee, H. M. *Astrophys. J.* **1984**, *285*, 89–108.
(26) Hillenbrand, R.; Knoll, B.; Keilmann, F. *J. Microsc.* **2001**, *202*, 77–83.
(27) Maghelli, N.; Labardi, M.; Patanè, S.; Irrera, F.; Allegrini, M. *J. Microsc.* **2001**, *202*, 84–93.
(28) Palik, E. D. *Handbook of Optical Constant of Solids*; Academic Press: New York, 1985.
(29) Kreibig, U.; Vollmer, M. *Optical Properties of Metal Clusters*; Springer-Verlag: Berlin Heidelberg, 1995.
(30) Scarpettini, A. F.; Bragas, A. V. *Langmuir* **2010**, *26* (20), 15948–15953.
(31) Frattini, A.; Pellegri, N.; Nicastro, D.; De Sanctis, O. *Mater. Chem. Phys.* **2005**, *94* (1), 148–152.
(32) Le Ru, E. ; Etchegoin, P. *Principles of Surface Raman Spectrosocpy*; Elsevier: Oxford, 2009; page 335.